

AISI 304 nitriding by PIII in DC toroidal plasmas

R. Valencia^{*}, R. López-Callejas^{*}, A. Muñoz C., S. R. Barocio, E. Chávez A., O. Godoy-Cabrera^{*}

*Instituto Nacional de Investigaciones Nucleares, Plasma Physics Laboratory
Apartado Postal No. 18-1027, Col. Escandón C. P. 11801, México D.F., México*

**Instituto Tecnológico de Toluca, Electronics Department,
Apartado Postal 50000, Toluca, México*

(Recibido 10 de octubre de 2003; Aceptado 15 de febrero de 2004)

Recent results obtained from the Plasma Immersion Ion Implantation (PIII) nitriding process on AISI 304 stainless steel by means of a DC toroidal plasma source of 0.23m and 0.08m major and minor radii, respectively, are reported. Among the main plasma parameters, electron densities in the range $1-4 \times 10^9 \text{ cm}^{-3}$ were established at an electron temperature between 0.5 and 2 eV. Nitrogen ions were extracted from the plasma and implanted in the steel substratum by means of a high voltage negative modulator operated at 5 kV, with 50 μs long pulses and a 1 kHz rate. This technology has achieved increments in the steel Vickers microhardness between 500 and 700 units at a 15 g load, according to the gas pressure. X ray diffraction (XRD) pattern confirmed the presence of the γ_N phase as a result of the nitriding process. Scanning Electronic Microscopy (SEM) indicated a 20 at.% increment in the nitrogen content of the implanted samples.

Keywords: Plasma immersion ion implantation; Nitriding; Stainless steel; Surface hardness

1. Introduction

The treatment of materials by means of ion implantation of 3D complex structures can be achieved at a low cost by Plasma Immersion (or PIII) technology, initially proposed by Conrad [1]. In the course of time, PIII has gained a considerable interest for material improvement applications in the manufacture of advanced industrial components such as metals, dielectrics and semiconductors [2-12]. PIII is a 3D ion implantation process which enables the surface treatment of samples with any geometry and relatively large sizes. During it, ions of a particular interest are extracted from the plasma by applying high voltage negative pulses in a repetitive way (typically, 1-100 kV, 10-100 μs long pulses at 10-1000 Hz frequencies) onto the sheath formed between the plasma and the sample to be processed. One of the main advantages of ionic implantation is its ability to be accomplished by the use of practically any kind of plasma source, from very low degree of ionization (10^{-6}) very low ion energy (10^{-1} eV) neutral vapor plasmas to those formed in a cathodic arc with energies in the tens or hundreds of eV and degrees of ionization in the order of 1, not to mention RF or ECR plasmas, thermoionic glow discharge plasmas, DC source plasmas, and so forth [13].

In the present study, some results obtained from the hardness raising of AISI 304 stainless steel after PIII nitriding at three different gas pressures between 10^{-1} to

10^{-3} mbar during 5 hours are presented. Results from the measurement of the implantation depth, the atomic percentage of implanted nitrogen, as well as the composition of the expanded phase achieved with our DC toroidal plasma source are included.

2. Experimental set up for the PIII process

For the toroidal plasma source we have chosen a highly stable DC glow discharge device in a long pressure interval. It is depicted in figure 1 along with the current PIII set-up, including diagnostic probe and the high voltage pulse supply systems. The toroidal plasma is created in a toroidal chamber assembled from four AISI 316 stainless steel sections of similar size, 0.08 m of minor radius and 0.23 m of major radius. interconnected with VitonTM seals and evacuated by a 500 l/s turbomolecular vacuum system allowing 10^{-7} mbar base pressures. The chamber is endowed with 35 ports providing great versatility for the diagnosis and general handling of the samples.

A 2.5 cm diameter positively biased cylindrical electrode, 15 cm in length, generates an electric discharge plasma to/from the negatively biased chamber wall thanks to a DC source 0-1500 V/2 A. The operational voltage was set at 900 V and the gas pressure was varied in order to achieve a smooth discharge which took place around 2×10^{-1} mbar. Once the discharge has been established, the work

Table 1. Results from microhardness, SEM and profilometry tests.

Pressure (mbar)	Microhardness (HV)	R _a (nm)	γ_N (1,1,1) (A.U.)	Nitrogen (at.%)	Depth (μm)
1.0×10^{-1}	740	70	122.4	38.89	4.63
1.0×10^{-2}	658	50	32.54	22.36	3.63
1.5×10^{-3}	473	40	22.06	17.65	1.12

^{*}e-mail: rva@nuclear.inin.mx

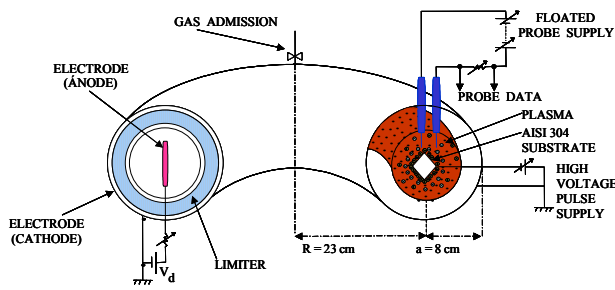


Figure 1. Cross sectional view of the toroidal chamber, displaying the DC supply, plasma, probe and high voltage pulse supply.

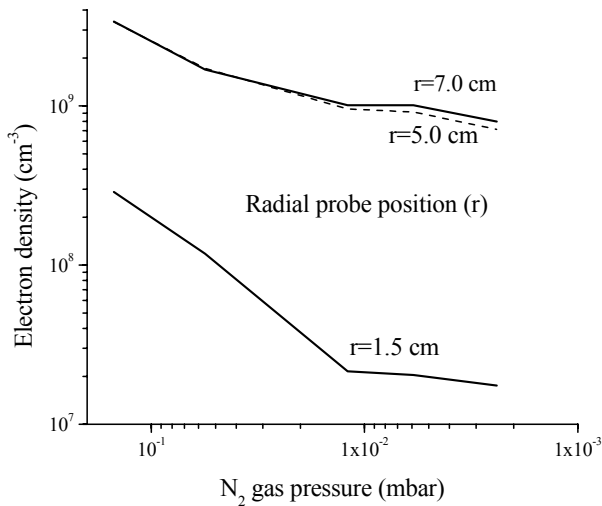


Figure 2. Radial variation of the electron density with respect to the nitrogen gas pressure at three radial positions of the probe.

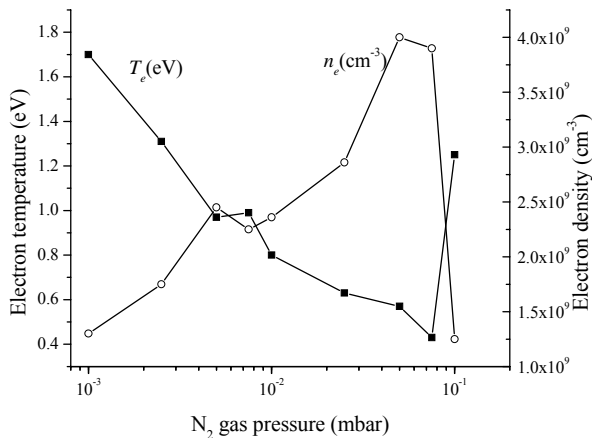


Figure 3. Dependence of the plasma density and temperature on nitrogen gas pressure

pressure can be selected, in the present case, between 1×10^{-1} to 1×10^{-3} mbar. Previously, the sample is introduced by means of a high voltage feedthrough and it is connected to the high voltage pulse generator, this was designed and built in our laboratory for such purpose [14]. The plasma thus produced reached electron densities in the range $1-4 \times 10^9 \text{ cm}^{-3}$ and electron temperatures of 0.5- 2 eV with high stability for long operation times ($>24 \text{ h}$). We typically run the discharge at powers between 90-150 W according to the gas pressure. In this way, the typical response of the system with respect to pressure implies voltages/currents of 380 V/370 mA for 1×10^{-3} mbar, lowering to 320 V/300 mA for 2.5×10^{-2} mbar and then raising again to 350V/420mA for 1×10^{-1} mbar.

3. Plasma characterization

The plasma produced in the toroidal chamber was extensively characterized both in density and temperature by means of double electric probes [15]. These were built from tungsten wire with 0.5 mm of radius, 5 mm of longitude and a 2 mm gap between the wires. The wires were encased in a low evaporation rate 4.5 mm diameter ceramic tube [16] by means of two perforations. The opposite extreme of the tube was tight sealed with Torr-seal™ resin in order to keep the probe in a high vacuum, while allowing it to be radially displaced within the plasma column.

Figure 2 shows the behavior of the electron density at three fixed probe locations (radially displaced from its initial position at the periphery of the vacuum discharge) as a function of the gas pressure in a nitrogen plasma. In this figure it is evident the tendency of the density to decrease with the pressure. Bearing in mind that the radial distance (r) is measured from the periphery to the center of the vacuum vessel, it follows that the density is lower near the wall.

The behavior of the electron density and temperature of the toroidal plasma at different nitrogen gas pressures is portrayed in figure 3. Our results seem to be in good agreement with the typical behavior of density and temperature reported in [17, 18]. As far as the efficiency in the implantation relies on a high ion current density, higher plasma density values are essential to the process. On the other hand, electron temperature, and therefore electron thermal energy, are far less relevant, which may be the case of the low T_e levels observed in figure 3. The sudden drop in the electron density at the narrow band of pressures higher than 1×10^{-1} mbar can be attributed to a lesser degree of ionization in the gas.

4. Experimental outcome

AISI 304 stainless steel samples measuring $25 \times 25 \times 0.25$ mm underwent the PIII process after having been abraded and mirror polished. The plates were introduced to the nitrogen plasma by a high voltage feedthrough and then biased to -5 kV by way of 50 μs long pulses at a 1 kHz

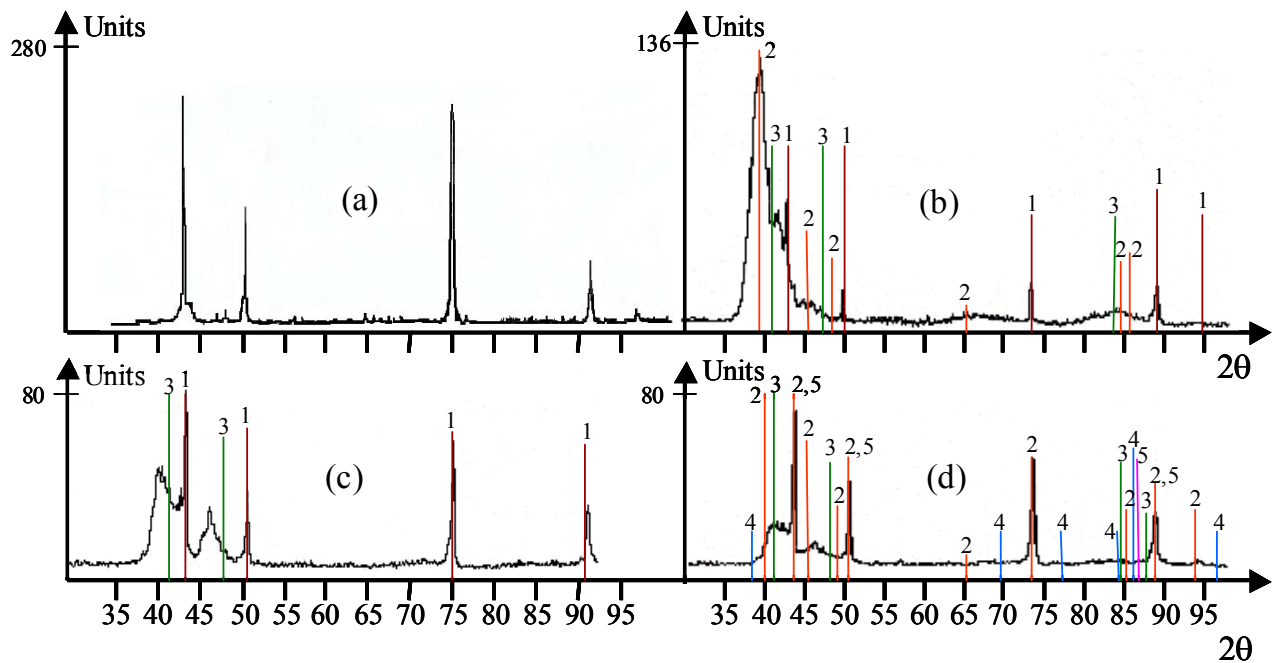


Figure 4. Diffractogrammes of: (a) untreated, (b) PIII treated at a 1×10^{-1} mbar gas pressure, (c) treated at 1×10^{-2} mbar, (d) treated at 1×10^{-3} mbar, AISI 304 stainless steel samples are presented. Label (1) refers to FeC, (2) refers to Fe_3N , (3) to Fe_3NiN , (4) to FeNiN, and (5) to CrFeNi.

frequency during 5 hours, operating at divers gas pressures, between 1×10^{-1} and 1×10^{-3} mbar. The results were evaluated by Vickers microhardness, X ray diffraction (XRD) and scanning electronic microscopy (SEM) techniques.

The samples that underwent the implantation process exhibited an evident increase in superficial roughness in agreement with Tian [10]. The roughening process results from grain boundary etching and distortion of the grains as a consequence of the high nitrogen content. So, above a 500°C sample temperature, an increase in the surface roughness usually accompanies the transition of the high N f.c.c phase to the b.c.c ferritic structure and CrN precipitation as established in [19, 20].

The outcome of our microhardness tests for a 15 g load are displayed in table 1. These results point to a significant increase in the hardness of the surface due to the formation of nitrides during the implantation of nitrogen ions into the iron matrix, provided that the microhardness measured 236 units prior to the processing. As shown in table 1, microhardness increases are associated with those of roughness R_a .

In figures 4(b)-(d) the X ray diffractogrammes taken from the nitrated samples as well as from the untreated one, 4(a), are presented. It follows from figures 4(b)-(d) an increase, due to a higher gas pressure, of the cubic phase characterized by a face centered geometry (austenitic γ phase) which becomes expanded by the implantation of nitrogen (γ_N phase). A similar behavior is exhibited by the Vickers microhardness (cf. table 1). The analyses were carried out at 2θ values between 30° and 100° , whose pattern clearly showed the presence of the expanded γ_N

phase shifted to lower angles to the angles: 43.4° , 50.6° , 74.5° , 90.5° and 95.7° from untreated sample. At several similar angles the following nitrides: FeNiN (roaldite), Ni_4N , FeNiN and Fe_3N were also identified.

A quantitative chemical analysis of the implanted substrata is essential to evaluate the efficiency of any PIII process. In our case, the scanning electronic microscopy (SEM) technique was applied by means of a PHILIPS® XL30 equipment. Table 1 exhibits the obtained results in terms of relative abundance and parameterized by different nitrogen gas pressures, within a 2% associated uncertainty margin.

In order to measure the depth of the implanted substrata, the samples were cut in a cross sectional way; the results are shown in table 1 where a tendency in the microhardness to grow with respect to the implant depth is evident.

5. Conclusions

It is observed that the plasma is denser toward the center of the toroidal vacuum chamber than at its periphery so that the present study clearly suggests the optimum location for the workpiece to be placed in order to be implanted.

Denser plasmas have been accomplished at higher gas pressures which indicates that the processes resulting from collisions in the ionic matrix (sheath) are not playing a significant role in the success of the implantation while, at the same time, such high pressure and density entail a considerable increment in the microhardness of the steel. The latter can be attributed to the relative expansion of the austenitic phase (γ_N) as well as the nitride formation detected by the XRD analysis. A monotonic correlation is

also found among roughness, microhardness and implantation depth within the variable ranges explored.

Acknowledgements

The present work was partially funded by CONACYT under contract 39676-Y and by COSNET under contract 642.02-P. The authors wish to thank the collaboration by M. T. Torres M. and I. Contreras V.

References

- [1] J. R. Conrad, J. L. Radtke, R. A. Dodd, F. J. Worzala, N. C. Tran, *J. Appl. Phys.* **62**, 4591 (1987).
- [2] B. Y. Tang, *J. Vac. Sci. Technol. B.* **12**, 867 (1994).
- [3] S. Qin, J. D. Berrnstein, Z. Zhao, Ch. Chan,, J. Shao, S. Denholm, *Nucl. Instr. and Meth. B* **106**, 636 (1995).
- [4] M. Ueda, C. Stellati, J. J. Barroso, M. C. A. Nono, A. Alexander, XVII th Int. Symp. On Discharges and Electrical Insulation in Vacuum, Berkeley, 603 (1996).
- [5] S.Y. Wang, P. K. Chu, B. Y. Tang, X. C. Zeng, Y. B. Chen, X. F. Wang, *Surf. Coat. Technol.* **93**, 309 (1997).
- [6] C. Blawert, B. L: Mordike, *Surf. Coat. Technol.* **116**, 352 (1999).
- [7] E. Menthe, K. T. Rie, *Surf. Coat. Technol.* **116**, 199 (1999).
- [8] M. Ueda, G. F. Gomes, L. A. Berni, J. O. Rossi, J. J. Barroso, A. F. Beloto, E. Abramof, H. Reuther, *Nucl. Instr. and Meth. in Phys B.* **161**, 1064 (2000).
- [9] E. Richter, R. Günzel, S. Parasacandola, T. Telbizova, O. Kruse, W. Möller, *Surf. Coat. Technol.* **128**, 21 (2000).
- [10] X.B. Tian, Z. M. Zeng, B. Y. Tang, T. K. Kwok, P. K. Chu, *Surf. Coat. Technol.* **128**, 226 (2000).
- [11] X. B. Tian, Y. X. Leng, T. K. Kwok, L. P. Wang, B. Y. Tang, P. K. Chu, *Surf. Coat. Technol.* **135**, 178 (2001).
- [12] X.B. Tian, P. K. Chu, *J. Vac. Sci. Technol. A.* **19**, 1008 (2001).
- [13] A. Anders, *Handbook of Plasma Immersion Ion Implantation and Deposition*, John Wiley & Sons, Inc., USA, (2000).
- [14] R. López-Callejas, R. Valencia A., A. E. Muñoz-Castro, O. G. Godoy-Cabrera, J. L. Tapia-Fabela, *Rev. Sci. Instr.* **73**, 4277 (2002).
- [15] O. Auciello, D. L. Flamm, Academic Press Inc., San Diego, CA, USA, **I** (1989).
- [16] Catalog of Coors Ceramics Company, "www.bioingegneria.uniba.it/bollettino"
- [17] H. Kojima, H. Kako, M. Terada, H. Sugai, T. Okuda, *Jap. J. of Appl. Phys.* **24**, 1432 (1985).
- [18] P. Chung-Hoo, S. Youl-Moon, L. Woo-Geun, *Thin Solid Films.* **312**, 182 (1998).
- [19] Samandi M., Shedden B. A., Smith D. I., Collins G. A., Hutchings R. and Tendys J., *Surf. and Coat. Technol.* **59**, 261 (1993).
- [20] Mändl S., Richter E., Günzel R. and Möller W., *Nucl. Instrum. And Meth. in Phys. Research B.* **148**, 846 (1999).